Research on Various Welding Methods on Aerospace Titanium Alloys: Collaboration between Akita University and AUT University

Timotius Pasang*, Yuan Tao*, Osamu Kamiya**, Yasuyuki Miyano**, Gakuya Kudo**

* Department of Mechanical Engineering, AUT University, Auckland, New Zealand 1020

**Department of Mechanical Engineering, Faculty of Engineering and Resource Science, Akita University,

1-1 Tegatagakuen-machi, Akita, 010-8502, Japan

tpasang@aut.ac.nz

Abstract: In the past two decades or so, titanium and its alloys have found a significant increase in the aerospace applications. One of the reasons is associated with the introduction of various new titanium alloys. Ti-5Al-5V-5Mo-3Cr (Ti5553) is one of the most notable new titanium alloys. This alloy has a high strength, excellent hardenability and good fracture toughness. Landing gear beam truck of aircraft has been successfully manufactured using this alloy. In order to find more applications in various areas, a number of factors are to be investigated, and one of them is its weldability. Three types of welding methods were used in this investigation, i.e. Laser Beam Welding (LBW), Electron Beam Welding and Gas Tungsten Arc Welding (GTAW). The results showed that it is possible to perform similar Ti5553 alloy weld as well as dissimilar titanium welds. It was observed that the (i) strength at the weld zones was lower compared with the base metal, and (ii) grains grew epitaxially from the near heat affected zone into the fusion zones. This study is part of a strong on-going collaboration projects between Akita University and AUT University.

Key words: Titanium alloys, electron beam welding, laser beam welding, gas tungsten arc welding

1 INTRODUCTION

Titanium and its alloys are used in many different areas such as aerospace, automotive, medical, sporting equipment and chemical industries. Such wide areas of applications are associated with the excellent high strength to weight ratio, good creep resistance, excellent corrosion resistance and good biocompatibility. A number new titanium alloys with comparable, if not better, properties were introduced in the last two decades or so. One of them is a metastable β titanium alloy known as Ti-5Al-5V-5Mo-3Cr (Ti5553) primarily for aircraft landing gear application [1]. Apart from its high strength, excellent hardenability and fracture toughness, this alloy also offers high fatigue resistance. A few other niche applications in the aerospace area have, since, been specified. For these applications, there may be a need to join them, e.g. by welding, and therefore its weldability needs to be investigated.

Depending on alloy classification, titanium and its alloys have moderate to excellent weldability [2]. Most titanium alloys have excellent weldabilty in the annealed condition, and relatively limited weldability in the solution treated and aged conditions [2]. In general, commercially pure titanium (CP Ti), α-titanium and α/β titanium alloys have better weldability compared with metastable β titanium alloys. These facts imply the effects of composition of the material and their conditions (e.g. strength). Aside from the materials, welding methods may have different influences on the weldability of titanium and its alloys [2]. It is generally accepted that fusion welding of titanium can successfully be performed in completely inert or vacuum environments either through arc or high-energy beam welding. Arc welding provides a high heat input into workpiece (and low power density of heat source), while the high-energy beam welding methods impart the opposite [3]. For this reason, the latter has the advantage of deeper penetration and much narrower weld zones, hence, thicker welds are possible compared with the former [2,3].

A summary of the microstructural features following welding of titanium and its alloys representing CP Ti, α/β alloys such as Ti6Al4V and metastable β titanium alloys are briefly

presented below. Typically, CP Ti welds have coarse columnar grains in the fusion zone (FZ) compared with the heat affected zones (HAZ) and the base metal (BM) [4]. The HAZ consists of equiaxed transformed β grains which increase in size as the FZ is approached. Within these grains, colonies of α-phases are present. The FZ of α/β alloys contains coarse, columnar prior beta grains. These grains may have originated from the near HAZ adjacent to the fusion line during solidification [2]. The grain structures of Ti6Al4V (Ti64) welds showed the presence of a small amount of acicular α, a larger amount of α-prime (martensite) in the HAZ and α-prime covering the entire FZ [5]. Huiquang et al. [8] reported columnar grains in the FZ. They also observed an increase in hardness due to the presence of α-prime in the FZ compared with the BM [6]. For metastable β titanium alloys, the FZ is comprised of coarse columnar β grains from solidification while the heat affected zone (HAZ) adjacent to the fusion lines are characterized by retained β structure. In this condition, they are low in strength (low hardness) but have good ductility. Becker and Baeslack [7] conducted weldability studies on three different types of metastable β titanium alloys (Ti-15V-3Cr-3Al-3Sn; Ti-8V-7Cr-3Al-4Sn-1Zr and Ti-8V-4Cr-2Mo-2Fe-3Al) and confirmed the above explanations. They also suggested that the alloys were weldable [7]. Liu et al. [8] studied the weldability of Beta-21S sheet using laser welding technique. They reported that the FZ and HAZ were narrow with fine retained β grain structures. Epitaxial grain growth was observed to form in the narrow HAZ through the fusion line into the FZ. The FZ had transitioned from a solidification mode of a cellular-type along the fusion line to a completely cellular-dendritic (or columnar dendritic) solidification mode at the weld centreline. Baeslack et al. [9] investigated Beta-C^{TM} alloy by implementing gas tungsten arc welding (GTAW) and observed epitaxial growth from the near-HAZ into the FZ, which solidified with a cellular mode and progressively formed a complete columnar-dendritic grain structure at the weld centreline. From the above summary, it can be seen that titanium may or may not be able to produce α-prime (martensite) upon cooling. This phenomenon is governed by the so called Molybdenum equivalent (Mo_{eq}). α-prime (martensite) could form if the Mo_{eq} is less than 10 [10].

The most common welding techniques to joint titanium and its alloys are gas tungsten arc welding (GTAW), gas metal arc welding (GMAW), plasma arc welding (PAW), laser beam welding (LBW) and electron beam welding (EBW) [2,11]. The first three methods fall in the arc welding category with high heat/energy input and low power density of the heat source, while the last two techniques belong to the high-energy beam group. In this study, similar and dissimilar titanium weld joints were made using EBW, LBW and GTAW methods. The results in terms of microstructures and mechanical properties are presented. However, due to the limit of this paper, only Ti5553/Ti5553 weld joints will be discussed in detail and the other types of weld joints are briefly explained.

2 EXPERIMENTAL

2.1 Materials

The main alloy studied was the new Ti-5Al-5V-5Mo-3Cr (Ti5553). Two other alloys, i.e. commercially pure titanium (CP Ti), Ti-6Al-4V (Ti64) were also used for comparison, all with a thickness of 1.7 mm. These materials represent three different classes of titanium, namely unalloyed (CP Ti), α/β alloy (Ti64) and β-alloy (Ti5553), respectively. Their chemical compositions are shown in Table 1. CP Ti and Ti64 alloys were commercially purchased, while the Ti5553 alloy was provided by the Boeing Commercial Airplanes.

Table 1. Chemical composition of the titanium alloys (wt.%)

Elements	CP Ti	Ti64	Ti5553
Ti	Bal.	Bal.	Bal.
Al	0.16	6.08	5.03
V	<0.01	3.85	5.1
Mo	<0.01	<0.01	5.06
Cr	<0.01	0.02	2.64
Fe	0.22	0.17	0.38
C	0.01	0.02	0.01
O	0.28	0.05	0.14
N	0.01	<0.01	<0.01

2.2 Welding Procedures

Full penetration butt joints were performed without filler metal (autogeneous) by LBW, EBW and GTAW. LBW was conducted at the Akita Research Institute of Advanced Technology (ARIAT), Akita - Japan, EBW was performed at the Air New Zealand Gas and Turbine facilities in Auckland, New Zealand, while GTAW was done at the Department of Mechanical Engineering, AUT University, Auckland, - New Zealand. The welding conditions are presented in Table 2. Various welding combination were made for similar titanium i.e. Ti5553/Ti5553, Ti64/Ti64 and CP Ti/CP Ti, and dissimilar titanium including Ti5553/Ti64, Ti5553/CP Ti, and Ti64/CP Ti.

Table 2. Welding parameters

Welding Methods	Parameters
LBW - Nd: YAG	Power = 2 kW; speed = 15 mm/sec; continuous argon gas flow of 20L/min
EBW	Voltage = 150kV; speed = 8.5 mm/sec; current = 3mA
GTAW	Current = 50 Amp DCEN; voltage 10V; continuous argon gas flow of 1-16L/min

2.3 Metallography and Microscopy

Metallographic samples were prepared according to the standard procedures. The steps consisted of grinding from 120 grit to 2400 grit SiC paper, polishing to 0.3 μm colloidal

alumina, followed by final polishing with 0.05 μm colloidal silica suspension. Kroll's reagent with a composition of 100 mL water + 2 mL HF + 5 mL HNO_3 was used to etch the metallographically-prepared samples to reveal the weld profiles and grain structures. Both optical microscope and scanning elecgtron microscope (SEM) were employed to characterize and study the microstructures of the etched samples.

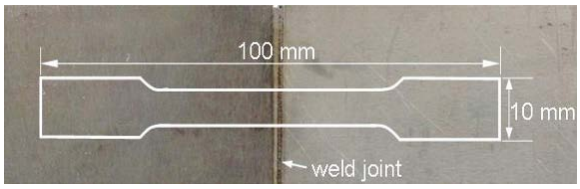

Figure 1: Schematic diagram showing a tensile test sample position on the laser beam welded (LBW) material.

2.4 Mechanical Testing

Mechanical testing performed including hardness and tensile tests. Vickers hardness method with a load of 300g (HV_{300g}) was used to investigate the hardness profile of the welds. Hardness indentations were placed about 0.2 mm from the top surface. Tensile tests samples were taken from the welded sheets (Fig.1) in accordance with ASTM E 8M – 04, with the weld located perpendicular to the tensile axis. Tensile tests were conducted at room temperature with a crosshead speed of 3 mm/min.

2.5 Post Welding Heat Treatment (PWHT)

Post welding heat treatment (PWHT) was performed on some of the welded samples at 700°C for 4h and air cooled. The specimens were then prepared metallographically, analysed and mechanically tested for comparison with the as-welded samples.

3 RESULTS AND DISCUSSION

Microstructures of the base materials of Ti5553, CP Ti and Ti64 are presented in Fig.2. The Ti5553 alloy showed a typical α/β microstructure with globular α particles distributed within the β matrix. These α particles have an average size of less than 5 μm. The CP Ti had nearly equiaxed α grains with an average size of 20 μm in the longitudinal direction. It also contained disperse β phase (dark). The presence of β phase is associated with the addition of small amounts of Fe in CP Ti. The Ti64 alloy had elongated primary α grains in the α/β matrix.

General weld profiles from EBW, LBW and GTAW are presented in Figs.3-7. It can be seen that the width of the weld zones of LBW and GTAW are markedly different, being fairly narrow in the former and could be up to five times wider in the latter. The grain sizes in the FZs for all welds were up to a few hundred microns. In the HAZ, large grains were observed at the near HAZ (along the fusion line) of up to 200 μm in the LBW samples, and up to 600 μm for GTAW samples. The larger grain sizes in the near HAZ are associated with intermediate peak temperature during welding that facilitates grain growth. The grains became gradually smaller towards the BM.

For Ti5553-Ti5553 weld joints (Figs.3-5), the difference in heat input appears to affect the size and shape of the weld profile but not the microstructure. The similarities were observed in the weldments' microstructures regardless of the welding method used as described in the followings:

1. The FZ contained a columnar dendritic-typed grain morphology indicating a high concentration of β-stabilizing elements,
2. The HAZ is decorated with retained, equiaxed β grains with larger grains at the fusion line and smaller grains towards BM,
3. Epitaxial grain growth from the HAZ into the FZ was clearly observed.

With regards to the weld shape, it was pointed out that the weld pool geometry is greatly affected by focus/defocus beam which may create a surface tension which is responsible for the metal flow, and hence, the weld zone shape [12]. The widening top and bottom surface, hence, hour glass-shaped is due to the presence of Marangoni convective currents which drives away the molten metal from the location of heat source [13]. There was another suggestion that the hour glass-shaped was due to heat flow in 3D and 2D on the surfaces and the mid-thickness, respectively [8]. The V-shaped in the GTAW is conduction dominated where the width of the weld is 2.5x the material thickness.

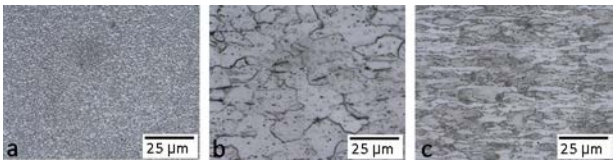

Figure 2: Micrographs showing microstructures of the BM for (a) Ti5553, (b) CP Ti and (c) Ti6Al4V.

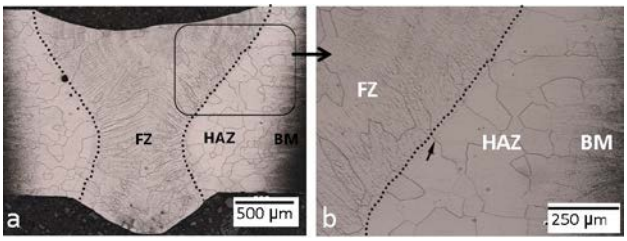

Figure 3: Micrographs showing examples weld profiles of Ti5553-Ti5553 EBW; dotted lines indicate fusion line, and small arrow indicate epitaxial grains

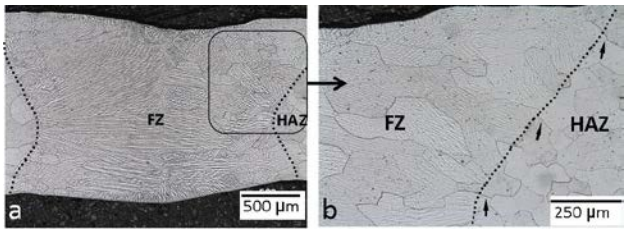

Figure 4: Micrographs showing examples weld profiles of Ti5553-Ti5553 LBW; dotted lines indicate fusion line, and small arrows indicate epitaxial grains.

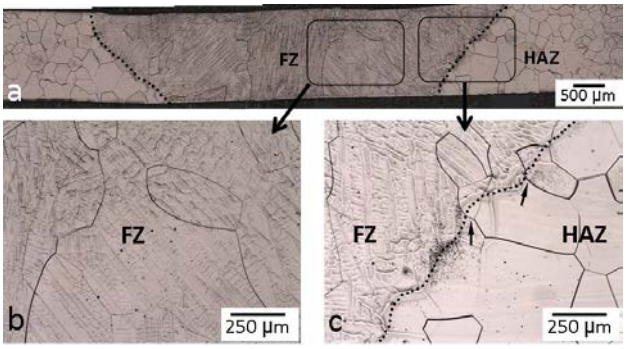

Figure 5: Micrographs showing examples weld profiles of Ti5553-Ti5553 GTAW; dotted lines indicate fusion line, and small arrows indicate epitaxial grains.

On the CP Ti-CP Ti weld joint, acicular α phases were observed from the HAZ to the FZ with larger grain size compared with the BM. In the FZ, with grain size of up to 200 µm, fine acicular α were evident. Note that fine acicular alpha can be mistaken for α-prime (martensite). For Ti64-Ti64 weldment, grains in the HAZ were slightly larger than those in the BM, and the grain size increased significantly in the FZ. α-prime (martensite) was faintly observed in the HAZ and is very clear in the FZ. The formation of martensite in Ti64 is associated with fast cooling rates from melting.

The microstructures for the dissimilar weld joints (Ti5553-CP Ti, Ti5553-Ti64 and CP Ti-Ti64) are summarised below: Ti5553-CP Ti, shown in Fig.6, for example, the presence of α-prime (martensite) at the FZ adjacent to the CP Ti side (not in the HAZ) is associated with the alloying elements coming from Ti5553. It was also observed that the amount of α-prime was decreasing towards the Ti5553; dendritic grains were observed on the Ti5553 side and lamellar type-grains were present on the CP Ti side; epitaxial grain growth was clearly observed on the Ti5553 side and less obvious on the CP Ti side.

On the Ti5553-Ti64 weld, α-prime (martensite) was clearly present at the Ti64 side from FZ through far HAZ. The presence of α-prime (martensite) was decreasing towards the Ti5553 side with the increase of the Mo_{eq} as explained later; dendritic grains were observed on the Ti5553 side and lamellar type-grains were present on the Ti64 side; epitaxial grain growth was observed on the Ti5553 side but not on the Ti64 side (Fig.7).

For CP Ti-Ti64 weld joint, the locations of the fusion boundaries were not very clear due to the similar microstructural features in the HAZ and FZ as well as the significant grain coarsening in the HAZ (which results in large β grains in this region). The presence of α-prime (martensite) was very clear on the Ti64 side but not on the CP Ti side.

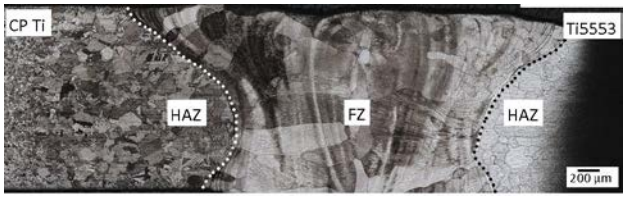

Figure 6: Micrographs showing an example of CP Ti-Ti5553 joint by LBW; dotted lines indicate fusion line.

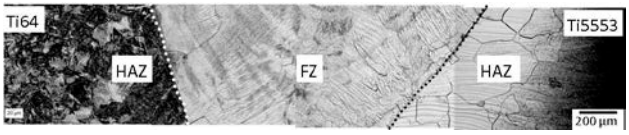

Figure 7: Micrographs showing examples of Ti64-Ti5553 weld joint by EBW; dotted lines indicate fusion line.

SEM micrographs showed dendritic-typed structures throughout the FZ of Ti5553-Ti5553. The extent of dendritic structures became less obvious on the FZ of Ti5553-CP Ti and Ti5553-Ti64 perhaps due to the formation of the martensitic phase. Epitaxial grain growth from the near HAZ into the FZ is very clearly observed (Fig.8). Figure 8b also indicates the presence of α-prime (martensite) in the Ti5553-Ti64 sample from the HAZ on Ti5553 side to the fusion line. The formation of both the dendritic-typed structures and α-prime (martensite) are compositional-driven. On the one hand, the higher the β stabilizing elements the more likely it is to form dendritic structures [3]. On the other hand, if the β stabilizing elements is too high, it will raise the Mo_{eq} which will inhibit the formation of α-prime (martensite) [10]. Ti5553 has Mo_{eq} of around 12.

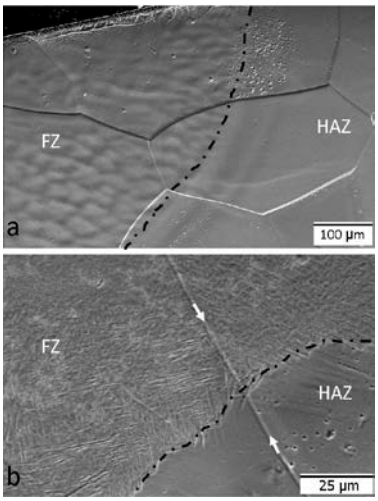

Figure 8: SEM micrographs showing fusion line area of (a) Ti5553-Ti5553, and (b) Ti5553-Ti64 at the near HAZ of Ti5553 side. White arrows indicate epitaxial grain boundary; dashed line represents fusion lines.

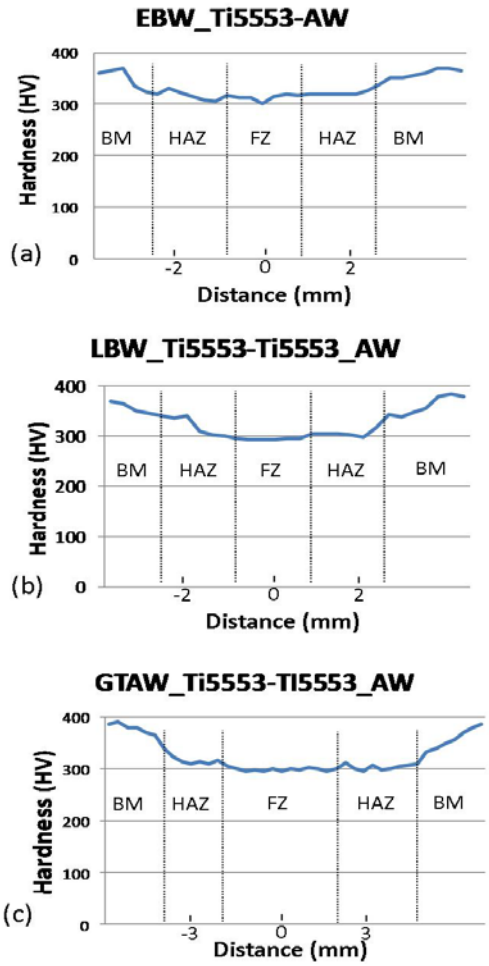

Figure 9: Hardness profiles of Ti5553-Ti5553 weld joints of EBW, LBW and GTAW

Hardness profiles of Ti5553-Ti5553 weld joints for EBW, LBW and GTAW are given in Fig.9. They showed a similar pattern i.e. lower hardness in the weld zones (both FZ and HAZ) compared with BM. The lower hardness in the weld zones is associated with the presence of retained β phase. Figure 10 shows an example of fracture surface from tensile test of a GTAW Ti5553-Ti5553 weld joint. Macroscopically, the fracture surface appears to be fairly brittle. However, at higher magnification, microvoid coalescence fracture mechanism (dimples) was obvious. This indicated a relative ductility at the weld zone.

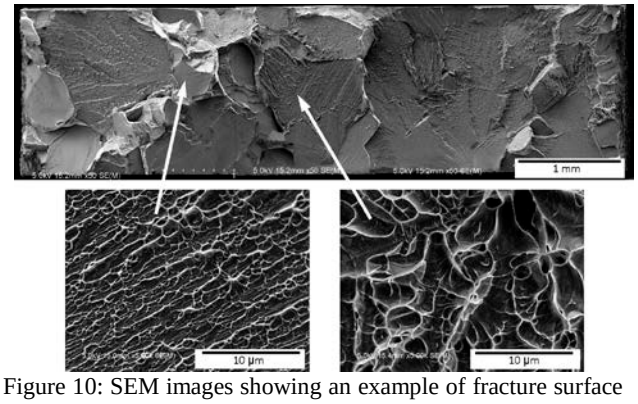

Figure 10: SEM images showing an example of fracture surface of tensile tested sample of GTAW Ti5553-Ti5553 weld joint

The effect of PWHT can be seen on Figs.11 and 12. Upon heating at 700°C/4h and air cooled, the microstructure had completely changed with the presence of homogeneous α precipitates in the BM, HAZ and the FZ (Fig.11). The fusion line is barely seen, but the grain structures are relatively obvious particularly the area between HAZ with equiaxed grains and BM with elongated grain structures (Fig.11).

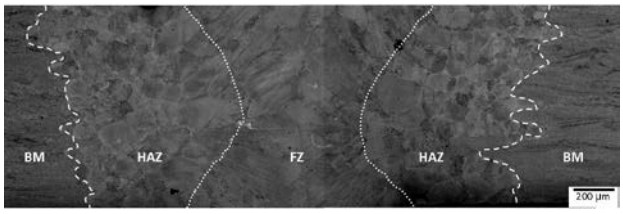

Figure 11: Micrographs showing an EBW profile after PWHT at 700°C/4h and air cooled.

Hardness values of the PWHT samples were constant across the BM to the HAZ and FZ (Fig.12). It also showed that hardness values of PWHT samples were comparable to that of BM in the as-received condition. Furthermore, the strength, both yield and ultimate, showed an increased by about 15 and 10%, respectively (Table 3). EBW and GTAW samples had lower strengths compared with LBW, possibly due to underfill on EBW and larger weld zone on GTAW. All samples presented in Table 3 fractured at the weld zones, while the welded samples involved CP Ti, fractured at the CP Ti BM.

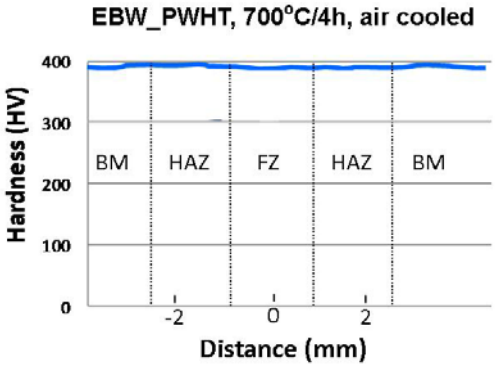

Figure 12: Hardness profiles of EBW sample following PWHT at 700°C/4h and air cooled.

Table 3. Tensile testing data of Ti5553-Ti5553 weld joints

Welding Methods	Yield Strength (MPa)	Tensile Strength (MPa)	Elongation (%)
EBW_AW	680	780	9
LBW_AW	1028	1053	12
GTAW_AW	785	785	8
EBW_PWHT	815	858	13

AW = as-welded; PWHT = post-weld heat treatment

4 SUMMARY

The three welding methods employed (LBW, EBW and GTAW) were able to perform similar Ti5553-Ti5553 but joint as well as dissimilar joint with CP Ti and Ti6Al4V alloys. The weld profiles of LBW and EBW showed an hour glass-like

appearance, while the GTAW samples had a common V-liked shape. Hardness values of the as-welded Ti5553-Ti5553 samples showed lower hardness (strength) at the weld zones. Following PWHT, the hardness values and tensile strength were restored to the same level of the BM.

Acknowledgement – The authors would like to thank Mr Richard Ison and Barry Able from the Air New Zealand for supporting the EBW, Mr. Kimura of the Akita Prefecture Research Center for performing the LBW and Mr. Makirai Henry for performing GTAW.

References

[1] Fanning, J.C., "Properties of Timetal 555 (Ti-5Al-5Mo-5V-3Cr-0.6Fe)", Journal of Materials Eng. and Performance, **14(6)**, 788-791, (2005).

[2] Donachie, M.J., "Titanium: A Technical Guide", second edition, ASM International, (2000).

[3] Sindo, K., "Welding Metallurgy", John Wiley and Sons, second edition, (2003).

[4] Lathabai, S., Jarvis, B.L and Barton, K.J., "Comparison of Keyhole and Conventional Gas Tungsten Arc Welds in Commercially Pure Titanium", Materials Science & Eng, **A 299**, 81-93, (2001).

[5] Irisarri, A.M., Barreda, J.L. and Azpiroz, X.,"Influence of the Filler Metal on the Properties of Ti-6Al-4V Electron Beam Weldments. Part I: Welding Procedures & Microstructural Charac.", Vacuum **84**, 393-399, (2010).

[6] Huiqiang, W., Jicai, F. and Jingshan, H.,"Microstructure Evolution & Frac. Behaviour for Electron Beam Welding of Ti-6Al-4V", Bull. of Materials Sci. **27,** 387-392, (2001).

[7] Becker, D. and Baeslack III, W.A., "Property - Microstructure Relationships in Metastable-Beta Titanium Alloy Weldments", Welding Journal **59**, 85-93, (1980).

[8] Liu P.S., Hou K. H, Baeslack III, W.A. and Hurley,J., "Laser Welding of an Oxidation Resistant Metastable-Beta Titanium Alloy – Beta-21S". Titanium '92 (Froes F.H. & Caplan I, editors), TMS, 1477-1485, (1993).

[9] Baeslack III W.A., Liu, P.S., Barbis, D.P., Schley, J.R. and Wood, J.R.,"Postweld Heat Treatment of GTA Welds in a High-Strength Metastable Titanium Alloy-Beta-C™", Titanium '92, Science & Tech., F.H. Froes and I. Chaplan (eds), TMS, 1469-1476, (1993).

[10] Bania P.J., "Beta titanium alloys in the 1990's", In: Eylon D., Boyer R.R., Koss D.A (Eds.), TMS, Warrendale, PA, 3-14, (1993).

[11] Lütjering, G. and Williams J.C., "Titanium", Berlin Springer, 23-42, (2003).

[12] Walsh, C.A. 2012. Laser Welding – Literature Review. University of Cambridge, England.

[13] Rai, R., Burgardt, P., Milewski, J.O., Lienert,T.J., and DebRoy, T. 2009. Heat transfer and fluid flow during elect ron beam welding of 21Cr–6Ni–9Mn Steel and Ti–6Al–4V alloy. J. Phys. D: Appl. Phys. 42, pp. 1-12.